Observation of the Crossover to Strong Scattering of Acoustic Phonons in Densified Silica

E. Rat,[1] M. Foret,[1] E. Courtens,[1] R. Vacher,[1] and M. Arai[2]
[1]*Laboratoire des Verres, UMR 5587 CNRS, Université de Montpellier 2, F-34095 Montpellier, France*
[2]*Institute of Materials Structure Science, KEK, 1-1 Oho, Tsukuba 305, Japan*
(Received 16 February 1999)

Inelastic x-ray scattering is used to observe high frequency acoustic excitations in densified silica glass. Longitudinal acoustic phonons are seen up to an energy $\hbar\omega \approx 9$ meV, corresponding to a scattering vector $Q \approx 2.2$ nm^{-1}. At higher Q, the nature of the signal changes rapidly, indicating a crossover to strong scattering. The absence of spectral intensity near $\omega = 0$ shows that these excitations remain long-lived compared to what might be inferred from their apparent line widths.

PACS numbers: 63.50.+x, 61.10.Eq, 61.43.Fs, 78.35.+c

The nature of the vibrations in glasses at frequencies high up on acoustic branches is a question of considerable current interest. Near the origin of these branches, long wavelength phonons are insensitive to structural details, and plane waves of definite wave vector $\mathbf{q}$ propagate as in a continuum. Their attenuation increases with their frequency Ω, owing either to internal friction or to scattering by structural inhomogeneities. Friction leads to a *finite lifetime*, i.e., to homogeneous broadening, generally with a temperature-dependent linewidth, $\Gamma \propto \Omega^2$ [1]. In contrast, scattering does not prevent excitations from remaining *long-lived*, but plane waves become *inhomogeneously* broadened according to the Rayleigh law, $\Gamma \propto q^4$ [2]. Friction usually dominates at frequencies considered "low" for the present purpose, but which in hypersonic terms are high, up to the limit of pulse experiments near 1 meV [1]. On the other hand, the thermal conductivity $\kappa(T)$ of glasses exhibits a universal plateau for temperatures $T \sim 10$ K, corresponding to dominant phonons around 4 meV [3]. The onset of this plateau can be explained if for plane waves a law $\Gamma \propto \Omega^4$ took over at "intermediate" frequencies above $\sim$1 meV [4]. The plateau itself would signal a crossover to strong phonon scattering occurring at an Ioffe-Regel limit, $\Omega = \Omega_{\mathrm{co}} \sim 4$ meV, where Γ first becomes of the order of Ω. In the "high" frequency regime, $\Omega > \Omega_{\mathrm{co}}$, plane-wave propagation would cease entirely [5], and the modes could be labeled only by their eigenfrequencies Ω. In systems as homogeneous as glasses, if Ω_{co} can be reached at all [6], one would expect that excitations remain diffusive beyond that limit [7].

A spectroscopic confirmation of this scenario is still lacking. It would be of considerable interest, not only in itself, but also as it could provide indirect structural information at length scales where usual structural methods are inefficient for glasses. So far, at meV frequencies, the spectroscopy has been dominated by the "boson peak" (BP) [8], whose profile is nearly independent from the *scattering* vector $\mathbf{Q}$ (to be carefully distinguished from a phonon *wave vector* $\mathbf{q}$). In neutron scattering, the intensity of the BP varies mainly as Q^2, consistent with an incoherent scattering approximation [9]. In that case, it carries no direct information on the structure. This is also true for the BP observed in Raman scattering [8]. There are new experimental possibilities to observe *coherent* excitations in noncrystalline media (Brillouin scattering) at high-Q values. This has been done both with inelastic neutron [10] and inelastic x-ray [11] scattering (IXS). Many Letters reporting IXS from glasses appeared over the past years. The spectra $S(Q, \omega)$, where ω is the running frequency, were generally adjusted to the damped harmonic oscillator function (DHO) [11]. This model *implies lifetime broadening* of plane waves with $q = Q$. Our previous spectroscopic work, in particular on vitreous silica, v-SiO_2 [12], and glassy selenium [13], established that the occurrence of an Ioffe-Regel crossover provides an alternative interpretation, that agrees with the observed $\kappa(T)$. However, Ω_{co} hardly exceeds 4 meV in most materials. For v-SiO_2 this leads to a crossover wave vector $q_{\mathrm{co}} = \Omega_{\mathrm{co}}/c_0 \simeq 1$ nm^{-1}, where c_0 is the sound velocity. This happens to be the lowest accessible limit for Q in current IXS. Further, with the posted instrumental resolution of $\sim$1.7 meV full width at half maximum (FWHM), and with a Lorentzian-like instrument profile, features below $\sim$4 meV in v-SiO_2 are very much masked by the wings of the intense elastic signal [14]. The present IXS experiments on densified silica glass, d-SiO_2, were undertaken to circumvent these experimental limitations.

Silica can be permanently densified when subjected to high pressures, as known for a long time [15]. The sample used here had been densified at $\sim$1000 K and 8 GPa [16]. Its density is $\rho \approx 2.62$ g/cm^3, much above that of v-SiO_2, $\rho = 2.20$ g/cm^3, and near that of crystal quartz. Intuitively, one expects that the range of inhomogeneities is strongly reduced by densification, and hence that q_{co} and Ω_{co} are larger in d-SiO_2 than in v-SiO_2. An increase in Ω_{co} is suggested by the $\kappa(T)$ data. The plateau is around 20 K in d-SiO_2 [17], indicating that Ω_{co} should be roughly twice that of v-SiO_2 where the plateau is near 10 K [4]. Also, the disturbing signal from the elastic structure factor, $S(Q, 0)$, should be reduced considerably

compared to that in v-SiO_2 [16]. For these reasons, we anticipated that the crucial region below and near Ω_{co} might be accessible to spectroscopy in d-SiO_2 using current IXS capabilities.

The experiment was performed on the IXS beam line (BL21-ID16) [11] at the European Synchrotron Radiation Facility in Grenoble, France. The final filtering of the incident x-ray beam is achieved using a Si(11 11 11) monochromator near back reflection, corresponding to an energy of 21 748 eV. The sample is placed in our evacuated oven with elongated arms minimizing the stray scattering by air. The scattered photons are collected on five analyzers, working on the same Si reflection. The ω sweep is achieved by scanning the monochromator temperature. The overall resolution, slightly different for each detector, was found to be around 1.9 meV FWHM at best. The analyzers are placed at fixed relative positions on an arm that can be rotated to change the scattering angles. In a configuration where the direct beam aims between analyzers 1 and 2, typical values of Q are 2, 1, 4, 7, and 10 nm^{-1}, for detectors 1 to 5, respectively. The scan durations were typically 3 to 5 h, and several scans were added to obtain one spectrum. Empty cell spectra accumulated 400 min revealed no detectable elastic signal. This gave an accurate determination of the mean detector backgrounds, which were subtracted from all spectra and instrumental functions prior to analysis. All spectra shown here are free of these backgrounds.

Prior to the IXS experiment, d-SiO_2 samples were characterized at room T by Brillouin light scattering (BLS) and refractive index measurements. The velocity of longitudinal acoustic (LA) phonons is a strong function of densification [18]. For $\rho = 2.62$ g/cm^3 we find $c_0 \simeq 6900$ m/s, significantly higher than in v-SiO_2 ($\simeq 5900$ m/s). A sample of the same density as that used in IXS was also investigated in function of T, to determine the relaxation of the densification with time. BLS offers a convenient method to do this *in situ*. Up to 300 °C, no relaxation of c_0 was observed over periods of several days. From 400 °C, a very slow relaxation appeared, with a time constant well over a week. Hence, $T = 575$ K was selected for the IXS experiment, as a good compromise between sample stability and inelastic signal strength. BLS was repeated on that sample after the IXS experiment to confirm that it did not relax.

Figure 1 shows a typical d-SiO_2 spectrum at $Q = 2.5$ nm^{-1}, accumulated for $\sim$20 h, on a 2.2 mm thick sample. Although the signal is weak, one easily recognizes the inelastic features above the wings of the elastic line. Useful inelastic spectra were obtained at 1, 1.3, 1.7, 2, 2.5, 4, 4.3, 7, and 7.3 nm^{-1}. A calibration was also performed on a 1.9 mm thick v-SiO_2 at the same T. The Stokes and antiStokes sides were added before analysis. Results at 4.1 and 7.1 nm^{-1} in Fig. 2 are the sum of data obtained at 4 and 4.3, or 7 and 7.3 nm^{-1}, respectively. This is fully justified as the Q dependence is very slow for sufficiently large Q.

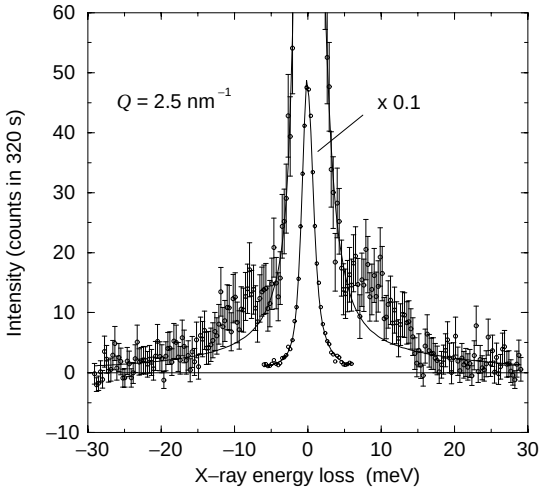

FIG. 1. Typical x-ray Brillouin spectrum of d-SiO_2. The solid line is the instrumental function smoothed with a spline and matched to the peak of the spectrum. The detector background is subtracted as explained in the text.

The inelastic signals were adjusted to several models. In all cases, the experimental signals were fitted to the sum of an elastic peak of adjustable intensity, plus the convolution of the instrumental function with the selected $S(Q, \omega)$. An exact account was taken of the Stokes–antiStokes asymmetry, as well as of the asymmetry in the instrumental function. What is shown in Fig. 2 is the

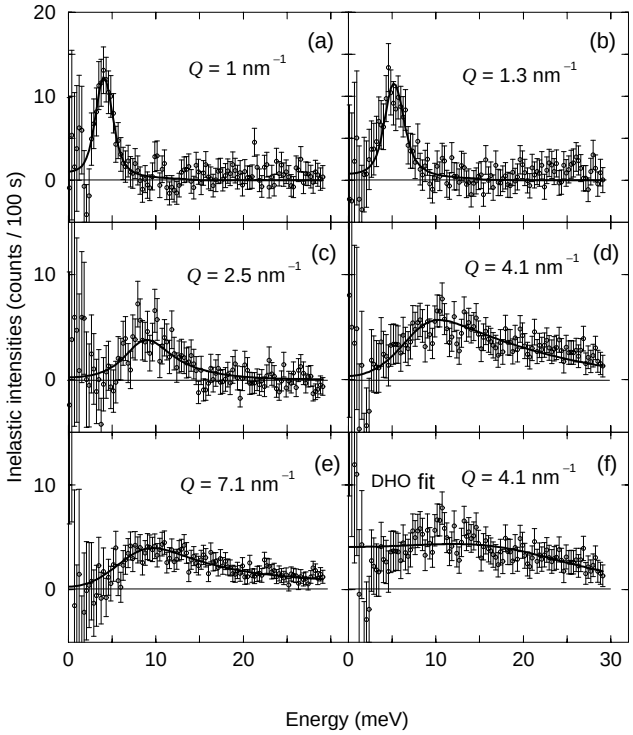

FIG. 2. Examples of a few inelastic spectra. The solid lines in (a)–(e) are obtained from fits with the crossover function [(1)–(3)] as explained in the text. For comparison, (f) is obtained from the same spectrum as in (d), but fitted to the DHO model.

remaining inelastic part, after subtraction of the fitted elastic contribution. It is clear that signals at small Q (from 1 to 2.5 nm^{-1}) can be adjusted either to a Lorentzian or to a DHO. Fitting to a Lorentzian, and taking into account the broadening due to the finite aperture of the analyzers, one finds no measurable width from 1 to 2 nm^{-1}. At 2.5 nm^{-1}, one finds $\Gamma_L = 1.2 \pm 0.4$ meV for the half-width, with a frequency $\Omega_L = 9.1 \pm 0.3$ meV. In all these fits, no adjustable background is needed, indicating that the subtraction of the detector backgrounds is fully adequate. The frequencies $\Omega_L(Q)$ of the Lorentzian fits are shown in Fig. 3(a). The line is the extrapolation of the low-frequency LA velocity measured in BLS. One notes that at these Q values the acoustic phonons already enter into a nonlinear dispersion regime. Beyond $Q = 2.5$ nm^{-1}, the broadening increases very fast, and the spectra at 4.1 and 7.1 nm^{-1} can be fitted neither to a Lorentzian nor to a DHO.

The failure of the DHO at 4.1 nm^{-1} is illustrated in Fig. 2(f), where the best DHO fit is shown. A similar result is obtained with the 7.1 nm^{-1} spectrum. For such broad lines, the DHO has considerable intensity at $\omega = 0$. This is a direct consequence of the model, as the intensity at $\omega = 0$ results from the assumed exponential decay of the correlation function at long times. The experimental spectrum shows a peak around 10 meV, but it decays to near zero at low ω. To adjust the DHO, the fit tries to subtract less elastic central peak in order to raise the inelastic contribution at low ω. However, it is not able to compensate for the low-ω dip, for two combined reasons: (1) 10 meV is well above the experimental resolution, and (2) the elastic peak is not strong, so that the absolute statistical error is smaller than the amount to be compensated. The situation was different in v-SiO_2, the spectral peak being near 5 meV, and the elastic signal being much stronger. This last point is seen from Fig. 3(b), which shows the relative elastic intensities we obtained for v-SiO_2 and d-SiO_2.

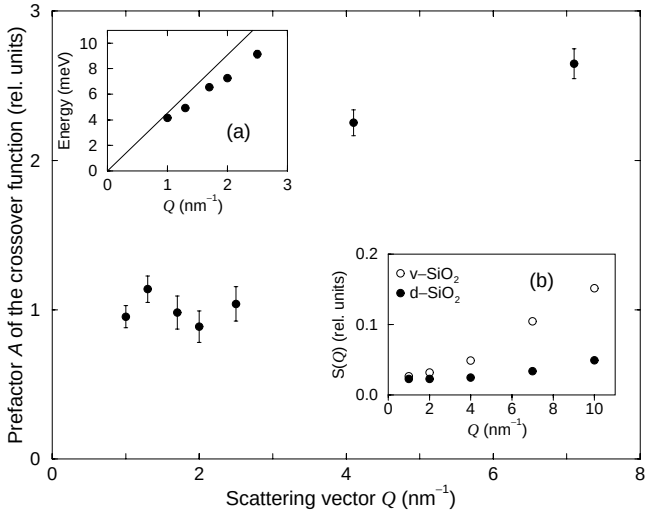

FIG. 3. The prefactor A of Eq. (1) resulting from fits as presented in Fig. 2. Inset (a) shows the values of Ω_L for Q up to 2.5 nm^{-1}, as discussed in the text; the solid line corresponds to the BLS velocity. Inset (b) compares the elastic scattering intensities obtained on both v-SiO_2 and d-SiO_2 for the same illuminated masses and corrected for absorption.

The fact that the signals in Figs. 2(d) and 2(e) decay to near zero for $\omega = 0$ shows that the excitations are much longer-lived than the widths of the spectra might suggest. Hence, we use as an alternate model a spectral function, $F(Q, \omega)$, that implies a crossover to strong scattering [19]. This produces the excellent fits shown by the solid lines in Figs. 2(a)–2(e). The $F(Q, \omega)$ which is used derives from an effective-medium-approximation (EMA) treatment of the vibrations of a *scalar* disordered system [19]. A similar expression was recently given for a nearly unstable vibrational model made of randomly coupled harmonic oscillators [20,21]. It was shown in that case that the EMA agrees well with simulation results. What $F(Q, \omega)$ describes is the projection on the Fourier component **Q** of modes that are *long-lived* but randomly scattered by disorder, so that **q** is not a good quantum number for $Q \geq q_{co}$. Neglecting Debye-Waller effects, the structure factor is given by

$$S(Q, \omega) = A(n_B + 1)Q^2 F(Q, \omega), \tag{1}$$

where A is a constant amplitude coefficient, n_B is the Bose population, and Q^2 results from the direct coupling of the x rays to density fluctuations, which applies to scattering from LA modes. The spectral function is [19]

$$F(Q, \omega) = \frac{c^2 Q^2}{\omega} \frac{\Gamma}{(\omega^2 + \Gamma^2 - c^2 Q^2)^2 + 4\Gamma^2 c^2 Q^2}. \tag{2}$$

In the spirit of the EMA [22], the complex self-energy is a function of ω alone, while q plays no role. This leads to ω-dependent damping, $\Gamma(\omega)$, and velocity, $c(\omega)$.

In the phonon limit, $Q < q_{co}$, $c = c_0$, and $S(Q, \omega)$ shows narrow peaks at $\Omega \cong \pm c_0 Q$. This is the "intermediate" regime of the introduction, where the narrow width of the peaks is given by $\Gamma \propto \Omega^4$, and thus $\Gamma(\omega) \propto \omega^4$ in (2). In the strong scattering limit, $\omega > \omega_{co}$, one expects the Ioffe-Regel criterion $\Gamma(\omega) = G\omega$, where G is a constant of the order of 1. That G is not necessarily 1 was already found in fitting BLS spectra of aerogels [23]. Less random systems tend to give a smaller G. This is confirmed by the simulation in [20] where systems further away from the instability also have a smaller G [24]. For $c(\omega)$, above Ω_{co} the EMA gives $c(\omega) \propto \omega^{1/2}$ [19]. To account for other dependences of the density of vibrational states on ω, this can be generalized to $c(\omega) \propto \omega^z$. In the crossover region, we use smooth empirical expressions [25],

$$\Gamma(\omega) = G \frac{\omega^4}{\Omega_{co}^3} [1 + (\omega/\Omega_{co})^m]^{-3/m}, \tag{3a}$$

$$c(\omega) = c_0 [1 + (\omega/\Omega_{co})^m]^{z/m}, \tag{3b}$$

where, m is a crossover exponent taking a large value for a sharp crossover. The spectral function (1)–(3), although partly empirical and necessarily approximative, gained respectability in being highly successful at describing nontrivial BLS spectra from strongly disordered aerogels.

The solid lines in Figs. 2(a)–2(e) were obtained with $m = 6$ (sharp crossover), $z = 0.5$ (EMA value), and $c_0 = 6200$ m/s to account for the local slope in Fig. 3(a). From the fits, we find $G = 0.34$ and $\Omega_{\text{co}} = 9 \pm 1$ meV. This corresponds to $q_{\text{co}} \approx 2.2\ \text{nm}^{-1}$. One also obtains relative values for the prefactor A in Eq. (1), as shown in Fig. 3. Up to $\sim q_{\text{co}}$, A is constant. The relative scattered intensities in v-SiO_2 and d-SiO_2, I_v and I_d, respectively, were compared using the data at $1\ \text{nm}^{-1}$ in both materials. For the same illuminated mass, and after correction for absorption, we find $I_v/I_d = 1.4 \pm 0.2$. This agrees perfectly with the theoretical Brillouin value of 1.34, giving confidence in the intensities. Beyond Ω_{co}, one sees in Fig. 3 a considerable increase in A. We interpret this as a shortcoming of the *scalar* EMA, which accounts only for LA modes [19,21]. At these $\mathbf{Q}$, the wave vector $\mathbf{q}$ having lost all meaning, the originally LA and TA (transverse) excitations all contribute to the scattering. The TA modes having smaller restoring forces, this effectively gives rise to an increase in A.

The value $\Omega_{\text{co}} \approx 9$ meV is to be compared to that in v-SiO_2, which at a similar T is $\approx$4 meV [12]. Since the crossover corresponds to the onset of strong scattering for all acoustic modes, it produces the plateau in $\kappa(T)$. As anticipated, the values of Ω_{co} agree with the relative positions of the plateaus in both materials [17]. Turning to the origin of the crossover, one sees from $S(Q, 0)$ in Fig. 3(b) that the structural fluctuations at the nm scale are considerably smaller in d-SiO_2 than in v-SiO_2. This presumably relates to the higher Ω_{co} of d-SiO_2. Also, the BP in d-SiO_2 is strongly depressed at small frequencies compared to that in v-SiO_2 [26]. Remarkably, Ω_{co} in both materials approximately corresponds to the maxima of the respective BP's. This is also found in the recent simulations [20]. It suggests that the strong scattering of acoustic modes is actually connected with the presence of an excess of other low frequency modes resonating with them. A similar conclusion results from the soft-potential model [27]. Clearly, the spectroscopy of d-SiO_2 ought to be pursued. For example, the data are not yet sufficient to decide whether the onset of the spectra at low ω and for $Q > q_{\text{co}}$ is in ω^2, as predicted by the EMA function used here [19], or in ω^4 as simpler phenomenological considerations might indicate [28]. However, the present experimental results now provide the first spectroscopic demonstration that there exists in glasses a crossover towards strong scattering of long-lived excitations.

The authors express their thanks to C. Masciovecchio for his invaluable expert assistance during the IXS measurements, to R. Vialla for the excellent design and construction of the evacuated oven, and to A. Cunsolo for further assistance with IXS.

[1] C. J. Morath and H. J. Maris, Phys. Rev. B **54**, 203 (1996).
[2] R. Truell, C. Elbaum, and B. B. Chick, *Ultrasonic Methods in Solid State Physics* (Academic Press, N.Y., 1969).
[3] J. E. Graebner, B. Golding, and L. C. Allen, Phys. Rev. B **34**, 5696 (1986).
[4] R. C. Zeller and R. O. Pohl, Phys. Rev. B **4**, 2029 (1971).
[5] S. Alexander, C. Laermans, R. Orbach, and H. M. Rosenberg, Phys. Rev. B **28**, 4615 (1983).
[6] S. Alexander, Phys. Rev. B **40**, 7953 (1989).
[7] J. Fabian and P. B. Allen, Phys. Rev. Lett. **77**, 3839 (1996).
[8] J. Jäckle, in *Amorphous Solids Low-T Properties*, edited by W. A. Phillips (Springer, Berlin, 1981), p. 135.
[9] U. Buchenau, N. Nücker, and A. J. Dianoux, Phys. Rev. Lett. **53**, 2316 (1984).
[10] J. Teixeira, M. C. Bellissent-Funel, S. H. Chen, and B. Dorner, Phys. Rev. Lett. **54**, 2681 (1985).
[11] F. Sette, M. H. Krisch, C. Masciovecchio, G. Ruocco, and G. Monaco, Science **280**, 1550 (1998), and references therein.
[12] M. Foret, E. Courtens, R. Vacher, and J.-B. Suck, Phys. Rev. Lett. **77**, 3831 (1996).
[13] M. Foret, B. Hehlen, G. Taillades, E. Courtens, R. Vacher, H. Casalta, and B. Dorner, Phys. Rev. Lett. **81**, 2100 (1998).
[14] M. Foret, E. Courtens, R. Vacher, and J.-B. Suck, Phys. Rev. Lett. **78**, 4669 (1997).
[15] P. W. Bridgman and I. Šimon, J. Appl. Phys. **24**, 405 (1953).
[16] Y. Inamura, M. Arai, N. Kitamura, S. M. Bennington, and A. C. Hannon, Physica (Amsterdam) **241B–243B**, 903 (1998).
[17] Da-Ming Zhu, Phys. Rev. B **50**, 6053 (1994).
[18] M. Grimsditch, Phys. Rev. Lett. **52**, 2379 (1984).
[19] G. Polatsek and O. Entin-Wohlman, Phys. Rev. B **37**, 7726 (1988).
[20] W. Schirmacher, G. Diezemann, and C. Ganter, Phys. Rev. Lett. **81**, 136 (1998).
[21] W. Schirmacher, G. Diezemann, and C. Ganter, Physica (Amsterdam) **263B–264B**, 160 (1999).
[22] I. Webman, Phys. Rev. Lett. **47**, 1496 (1981).
[23] E. Anglaret, A. Hasmy, E. Courtens, J. Pelous, and R. Vacher, Europhys. Lett. **28**, 591 (1994).
[24] Above Ω_{co}, $G \approx \lambda/4\pi l$, in the notation of Fig. 2 of [20], showing that G can be quite a bit smaller than 1 also in that case.
[25] E. Courtens, R. Vacher, J. Pelous, and T. Woignier, Europhys. Lett. **6**, 245 (1988).
[26] Y. Inamura, M. Arai, O. Yamamuro, A. Inaba, N. Kitamura, T. Otomo, T. Matsuo, S. M. Bennington, and A. C. Hannon, Physica (Amsterdam) **263B–264B**, 299 (1999).
[27] V. G. Karpov, M. I. Klinger, and F. N. Ignatiev, Sov. Phys. JETP **57**, 439 (1983).
[28] J. Jäckle and K. Froböse, J. Phys. F **9**, 967 (1979).